SIMULATING ARTIFICIAL LENSES OF FRESH GROUNDWATER IN DESERT CONDITIONS

A. YAKIREVICH[1, ✉], M. KUZNETSOV[1], S. SOREK[1] and I. MAMIYEVA[2]

[1]Department of Environmental Hydrology and Microbiology, Zuckerberg Institute for Water Research, Blaustein Institutes for Desert Research, Ben-Gurion University of the Negev, Sede Boker Campus 84990, Israel
E-mails: alexy@bgumail.bgu.ac.il, kmikhail@bgumail.bgu.ac.il, sorek@bgumail.bgu.ac.il,
[2]National Institute of Deserts, Flora and Fauna, Bitarap Turkmenistan str., 15, Ashgabat, 744000, Turkmenistan,
E-mail: sic@online.tm

Abstract

In desert areas clayey watersheds can be used for collecting runoff water during seasonal precipitation and infiltrating it into the saline water table. Thus, an artificial lens of fresh groundwater (ALFGW) can be created. A pilot system for ALFGW formation was constructed by the National Institute of Deserts, Flora and Fauna of Turkmenistan in the southern part of the Kara-Kum desert. Field experiments were conducted to study lens formation. We applied the FEFLOW code to simulate density driven flow and transport in the unsaturated-saturated zones. The model was calibrated with available field data. It was found that there is a relatively sharp interface between the ALFGW bottom and the saline groundwater, while changes of water salinity are much smaller within the ALFGW. The results of sensitivity analysis demonstrated that the ALFGW spatial extent (volume, thickness, and surface area) depends on soil parameters, groundwater salinity, characteristics of a recharging system, and on the infiltration regime. The ALFGW that is not replenished during more than one year decreases in thickness and increases in its area.

Keywords: saline groundwater, freshwater lens, mathematical model, density driven flow.

Introduction

In desert conditions, precipitation is often the main source of fresh water. Different methods can be used for collecting this water into natural or artificial surface storages, as well as by infiltrating it into the underground to refill groundwater resources. Collecting runoff water from clayey watersheds during and after rainstorms is relatively cheap and simple. Takyr (from Uzbek *takyr*, barren land) watersheds can be found in many world deserts. The takyr soil is mainly composed of clay particles; it has low hydraulic conductivity and a high runoff coefficient. A takyric horizon comprises a crust and a platy structured lower part. It occurs under arid conditions in periodically flooded soils.

✉ Corresponding author

Deserts occupy 80% of the Turkmenistan area. In the plane part of the country, groundwater mostly has high level of salinity (15-35 g/L), and the quality of the surface water has been significantly deteriorated because of non-sustainable agriculture. Takyr watersheds are being used for collecting runoff water during seasonal precipitation and infiltrating this water into the saline water table. Thus, an artificial lens of fresh groundwater (ALFGW) can be created and used afterwards for water supply. Actually, this method was implemented by ancients in Turkmenistan during centuries. However, the technology of lens formation and its exploitation was very inefficient: about 90% of runoff water was lost due to spatially scattered infiltration and evaporation, while only 10% of water replenished the ALFGW.

Natural lenses of fresh water were studied by Wentworth (1948), Lebbe (1983), van Dam (1999), however, mainly under dunes of coastal areas. In desert conditions ALFGW formation was studied, e.g., by Kunin (1959), Leshinsky (1970), Rogovskaya *et al.* (1986), Ganus and Kuznetsov (1992), and Mamieva (1999). It was found that the ALFGW has small thickness (3-10 m) and its transition zone between salt and fresh water is narrow (1-3 m). Conditions of ALFGW recharge and formation are very different from that of natural lenses. Therefore, it is important to study the process of the ALFGW formation and the dynamics of its water quality during lens exploitation.

In what follows we present the results of field observations and simulations of density driven flow and solute transport in the unsaturated and saturated zones during the ALFGW formation.

Experimental observations

A pilot system for ALFGW formation was constructed in 1965 by the National Institute of Deserts, Flora and Fauna of Turkmenistan. The system located at the takyr Karrykul in the southern part of the Kara- Kum desert, 60 km to the north of Ashkhabad (Leshinsky, 1970). Mean annual precipitation is 150 mm and rains occur manly during winter-spring seasons. The catchment surface area is 1.75 km^2, which allows an annual collection of 20,000-25,000 m^3 of runoff water. The experimental pilot system consisted of the infiltration pond of 40x40 m at the bottom, 50x50 m at the top, and 3.3 m depth (Figure 1). The central part of the infiltration pond is occupied by an island (20x20 m at the bottom and 10x10 m at the top) where a cluster of boreholes was installed and used for observations of water levels and sampling groundwater from different depths. A number of monitoring boreholes were also drilled around the infiltration pond. In 1982, four recharging wells were constructed to enforce water infiltration, and a settling pond was excavated to decrease turbidity of runoff by sedimentation.

The upper 12 m of the unsaturated zone is built of fine and medium grained sand with lenses of sandy loam, loam and clay. Underneath this zone the aquifer is composed of well sorted coarse sand of the Kara-Kum suite (Rogovskaya *et al.*, 1986). Content of salts in the unsaturated zone varied in the range of 1–10 g/kg in the sand and 10–20 g/kg in the loam and clay layers. The aquifer base, at the depth of 30 m, is composed of clay deposits. Groundwater of sodium-chloride type has a salinity of more than 20 g/L TDS, and the depth of the water table is at about 15 m. Hydraulic conductivity of the sand in the saturated zone is 3.7-10.5 m/day. The groundwater flows towards the northwest driven by a gradient of 0.0002-0.0003. During the years 1965 to 1968, a volume of surface water of about 25,600 m^3 with salinity of 0.2 g/L, was infiltrated into the underground. This created a lens of a maximum thickness of 6 m and a radius of

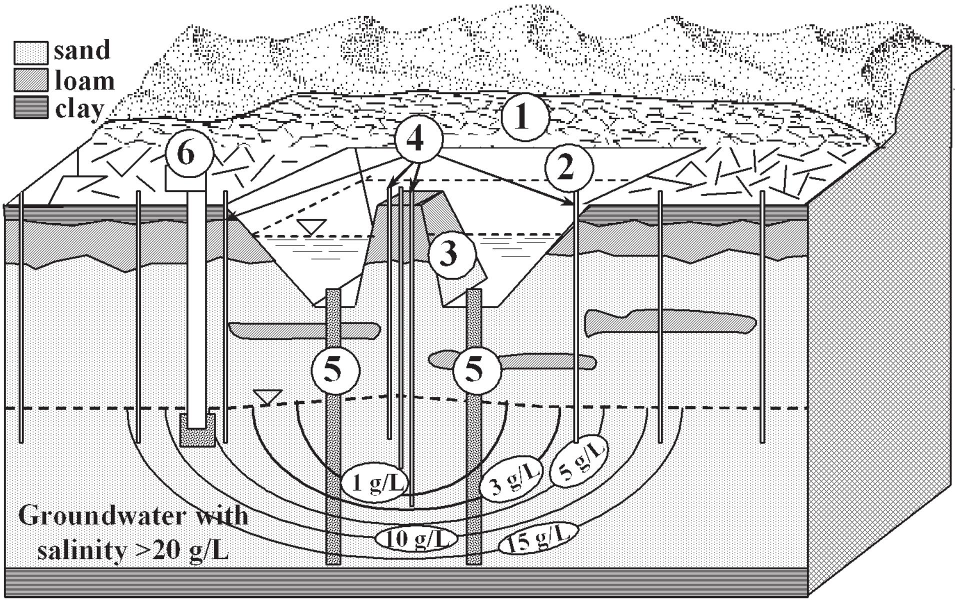

Figure 1. Experimental system for the ALFGW formation at the takyr Karrykul: 1- takyr watershed, 2-infiltration pond, 3- observation island, 4-observation boreholes, 5-recharging wells, 6-exploitation well.

38 m with concentration increasing from less than 2 g/L at the central part of the lens to 10 g/L at its periphery (Leshinsky 1970, Rogovskaya *et al*., 1986). It was also found that infiltration rate drastically decreased with time. The runoff water on the takyr soil has significant concentration of clay particles (3–8 g/L), sedimentation of which caused the sealing of the base and embankments in the infiltration pond, during water percolation. This sealing causing a decrease in hydraulic conductivity was accounted for when simulating the processes associated with the ALFGW formation. The simulation results and their comparison with field observations are presented in the *Results and Discussion* section.

Mathematical model

The process of the ALFGW formation was simulated using the FEFLOW numerical code (Diersch, 2002) for 2-D/3-D density driven flow and transport in the unsaturated and saturated zones. The non-linear Richards equation and advection-dispersion equation are coupled through the liquid density, which is assumed as a function of solute concentration. The balance equations of water flow and solute transport are solved using the finite-element method.

Infiltration of fresh water through the unsaturated zone is modeled by assigning water level varying with time at the infiltration pond surface. To account for the effect of water turbidity on infiltration rate through the pond bottom and its embankments, we developed a sub-model of soil particles sedimentation in the pond creating a layer ("cake") impeding water infiltration.

We assume that at an initial time (t_0) the pond is filled by water with a volume ratio of soil particles c_p, and a mean radius *r*. The vertical velocity (v_p) of clay particle sedimentation is estimated by Stokes law: $v_p=2gr(\rho_p-\rho_w)/9\mu$, ρ_p and ρ_w are bulk densities of particles and water, respectively, *g* is gravity acceleration, and μ is the dynamic viscosity. We also assume that during particle sedimentation, the thickness of water in the pond is divided by two zones: the upper zone with clean water, and the lower zone with particles volume ratio c_p. This assumption is similar to that introduced by Burger *et al*. (2001). The elevation (Z_G) of the moving boundary between these two zones from the pond bottom is defined by

$$Z_G = H_w - (v_p - E_0)(t - t_0) \quad (1)$$

where the transient water level in the pond (H_w) at time *t* is determined by the water balance equation that reads

$$\frac{\partial V(H_w)}{\partial t} = Q_{ro} - Q_{\inf} - S(H_w)E_0 \quad (2)$$

where $V(H_w)$ is the water volume in the pond, Q_{ro} is runoff inflow rate, $Q_{\inf} = \int_\Omega q_n d\omega$ is the infiltration rate (q_n) integrated over the pond wetted surface Ω, $S(H_w)$ is water surface area in the pond, and E_0 is the evaporation rate from water. In a case when infiltration is enhanced by the construction of recharging wells, the latter is accounted for by introducing additional sink terms into (2).

Velocity of clay particles (v_s) that are being settled out on the pond embankments and its bottom is composed of a the motion of particles shifted by Stokes velocity (v_p) and a liquid velocity normal to the pond surface (v_l): $v_s = v_l + v_p \cos(\mathbf{n},\mathbf{z})$, where axis **z** is directed upwards from the soil surface and **n** is an outward unit vector normal to the pond boundary surface. Thus, if we assume that a cake with a thickness of $b(x,y,t)$ having a uniform porosity, n_b, then the development of a cake due to particle sedimentation process is described by the following mass balance equation

$$(1-n_b)\frac{\partial b(x,y,t)}{\partial t} = [v_l + v_p \cos(\mathbf{n},\mathbf{z})]c_p \quad (3)$$

where *x* and *y* are planar coordinates (the origin is located at the center of the pond, axis *x* is directed eastward and axis *y* is directed northward). Note, that for the sake of simplicity, we do not account for the consolidation process of the cake and particles filtration (Burger *et al*., 2001), i.e. above the boundary separating clean water and water with particles (Z_G), cake thickness remains constant.

Since we neglected particles filtration, the volumetric flux of particles is zero below the upper cake boundary. At this boundary we assign the continuity of a volumetric flux for the liquid-particles mixture above, and clean water infiltrated through the cake below, to read

$$c_p v_p \cos(\mathbf{n},\mathbf{z}) + (1-c_p)v_l = q_n \quad (4)$$

where q_n is a normal water flux through the infiltration pond at the relevant boundary. Hence, the liquid velocity (v_l) can be estimated by (4).

Substituting (4) into (3) we obtain

$$(1-n_b)\frac{\partial b(x,y,t)}{\partial t}=\frac{c_p}{1-c_p}\left[q_n+v_p\cos(\mathbf{n},\mathbf{z})(1-2c_p)\right]\chi_{(Z_G-Z_{ip}-b\cos(\mathbf{n},\mathbf{z}))} \quad (5)$$

where $Z_{ip}(x,y)$ denotes the elevation of a spatial location (x,y) at the pond surface above the pond bottom and $X_{(Z_G-Z_{ip})}$ denotes the Heaviside function.

Expressions (1)-(3) and (5) were coupled with the FEFLOW model using the Cauchy boundary condition assigned at the infiltration pond wetted surface boundary

$$x,y,z,\ \varepsilon\ \Omega: \qquad -\mathbf{K}\cdot\frac{\partial\phi}{\partial\mathbf{n}}=q_n=-K_b\frac{H-\phi}{b} \quad (6)$$

where **K** is the hydraulic conductivity of soil, K_b is the mean hydraulic conductivity of the cake and $H=H_w-H_p$ denotes the pond piezometric head, H_p denotes depth of the pond and $\O$ denotes hydraulic head below the cake bottom. This condition simulates flux of water (q_n) infiltrated through the pond, depending on the cake thickness and its hydraulic conductivity.

The above (1)-(3) and (5) are solved numerically at each time step by a computer code that was developed and coupled with the FEFLOW code, using the C++ language and the FEFLOW programming interface.

In the developed model we do not account for the dispersion of the liquid phase and physico-chemical reactions between the solid and liquid phases, such as adsorption, ion exchange, precipitation-dissolution. Based on past 1-D simulations, the latter problem will be discussed in the following section.

Results and Discussion

A 3-D model of the ALFGW at the Karrykul experimental site

To simulate the ALFGW formation for a 3-D configuration, together with field observation data at the takyr Karrykul, the modeling domain was chosen to be a square area of 1000 x 1000 m and 30 m thickness. An infiltration basin was situated at the domain center, sizes of 40 x 40 m at the bottom, 50 x 50 m at the top, and 3.3 m in depth. A non-uniform finite element mesh was composed of 48887 nodes. The horizontal mesh dimension was finer (1 m) near the basin and increased to the extent of 80 m at the boundaries of the modeling domain. The vertical size of the mesh varied from 0.5 m at the top to 1 m at the bottom.

Initial piezometric head distribution was calculated by assuming vertical equilibrium conditions, and using observed values of groundwater level (15 m at the middle of the infiltration pond), known gradient of water table (0.0002), and groundwater flow direction (northwest). Calculations were based on the Boussinesq approach. Initial salinity of groundwater was prescribed as constant and equal to 22.5 g/L. In the unsaturated zone we assigned measured distribution of salt concentration varying with depth.

We assumed that water flow and transport regime in the saturated-unsaturated zone at a far distance from the pond was subject to steady-state regime and did not practically depend on the process of the lens formation. Therefore, Dirichlet boundary conditions for the flow and transport problems were assigned at the area borders.

At the soil surface, water flux (resulting from rain and evaporation) was prescribed everywhere excluding the pond where the Cauchy boundary condition (6) was prescribed. This condition accounts for the changing water level in the pond as a function of inflow, evaporation and infiltration through the impeding layer as described previously. The pond water salinity was equal to 0.2 g/L. To account for the effect of the observation island as a flow obstacle, a no flow boundary condition was assigned at a square of 10x10 m located at the pond center.

The unsaturated zone parameters (retention curves and the unsaturated hydraulic conductivity) were estimated using an indirect method based on particle size distribution data (Arya and Paris, 1981; Mishra *et al*, 1989) and the van Genuchten relations (1980). The saturated hydraulic conductivity (K_s) and porosity (n) of the different lithological units were estimated from data of field and laboratory experiments. Values of K_s were 7.0, 0.8, 0.4 and 0.1 m/day for coarse sand, fine sand, loam and clay, respectively, and the n values were 0.31, 0.41, 0.43 and 0.36, respectively. The longitudinal and transversal dispersivities of 0.5 and 0.05 m, respectively, were assessed by trial and error using limited data of groundwater salinity. Porosity and hydraulic conductivity of the cake were 0.96 and 1 mm/day, respectively. These values were adopted by fitting the observed and simulated water levels in the pond. Volume ratio of soil particles in runoff was 0.002 cm^3/mL, a mean radius was 0.005 mm.

Simulation period, following field experiments, from May 1965 to April 1970 was subdivided into several time intervals (infiltration cycles). At the beginning of each cycle, the pond was cleaned from sediments and filled with water collected at the watershed during rainstorms. The total water volume of 26,000 m^3 was infiltrated. An approximate of 5,000 m^3 of water was needed to saturate the vadose zone under the pond. During the first year, groundwater salinity slightly increased due to leaching of salts from the unsaturated zone. Continuing infiltration resulted in a decrease of groundwater salinity under the pond. Figures 2 to 4 show simulated distribution of groundwater salinity and the point values at the observation boreholes, for June 1967 and April 1970. Figures 2 and 3 demonstrate the areal distribution of concentrations at different depths, starting from $z = -15$ m (water table) in June 1967 and in April 1970, respectively. The ALFGW (area contoured by the iso-concentration 10 g/L) has the maximum extent at this depth increasing the radius from 26 m in 1967 (Figure 2) to 45 m in 1970 (Figure 3). The maximum thickness of the ALFGW was about 4.5 m in 1967 and it did not change in 1970 (Figure 4). We note (Figures 2 to 4) that concentration of salts at the ALFGW center is higher than at its vicinity because of the observation island, which prevents infiltration at the middle of the pond. Consistent agreement was obtained between the simulated and observed concentrations. However, at some locations (e.g. under the eastern side of the pond) the observed groundwater salinity is somewhat higher than what was simulated. This may be due to actual heterogeneity of the geological structure and the distribution of concentrations that were not introduced into the model. By 1970 the ALFGW slightly moved northwest in the direction of ambient groundwater flow (Figure 3). The ALFGW with concentration less than 10 g/L contains water volumes of about 2800 and 5200 m^3 in 1967 and 1970, respectively.

To estimate the effect of water-rock interaction resulting from physico-chemical reactions during leaching salts from the unsaturated zone into groundwater, we adopted a 1-D model of flow and multi-component transport. This model considers water flow and major ions transport in the unsaturated-saturated zones accounting for the cation exchange and dissolution-precipitation of gypsum and calcite (Yakirevich *et al.*, 1997). Simulations with that model indicated that cation exchange processes have minor effects on soil

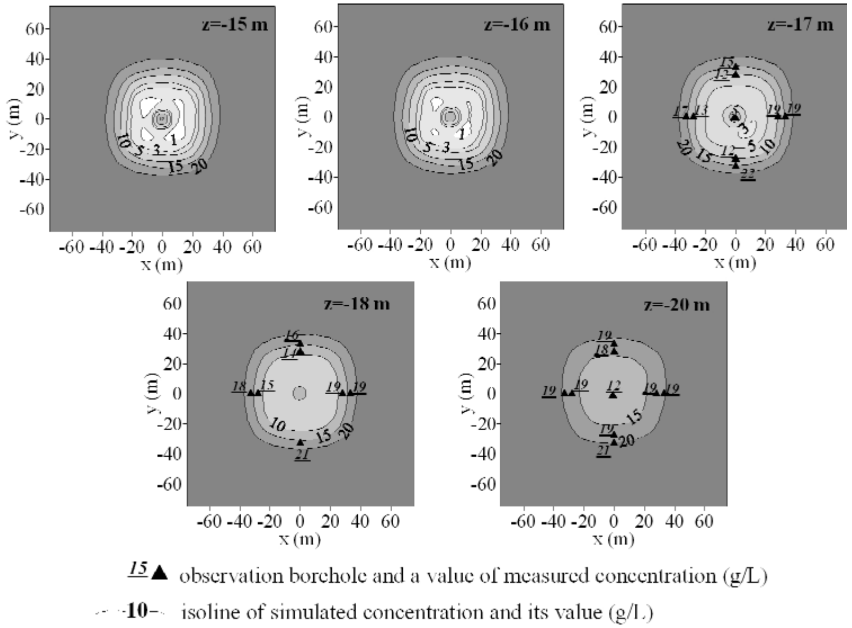

Figure 2. Measured and simulated areal distribution of concentrations at different depths in June 1967.

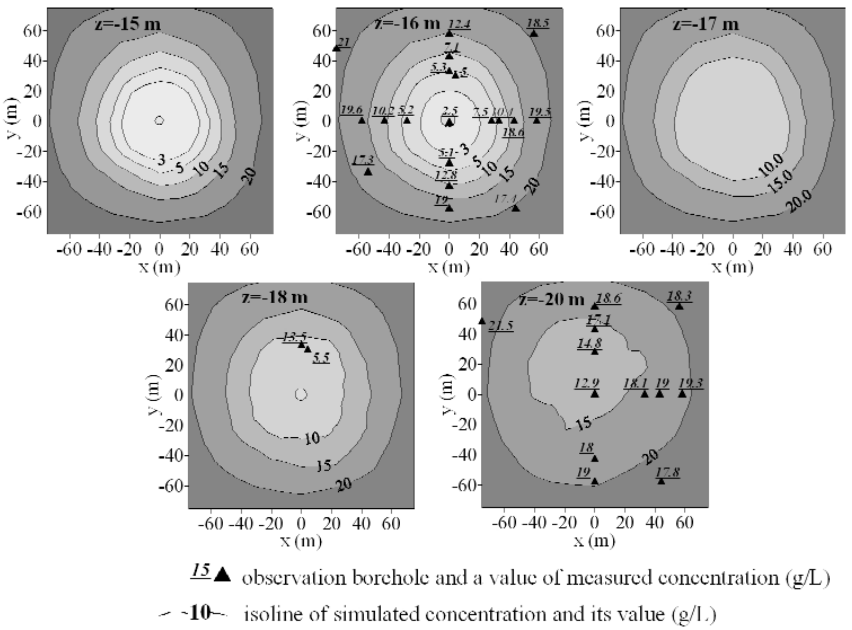

Figure 3. Measured and simulated areal distribution of concentrations at different depths in April 1970.

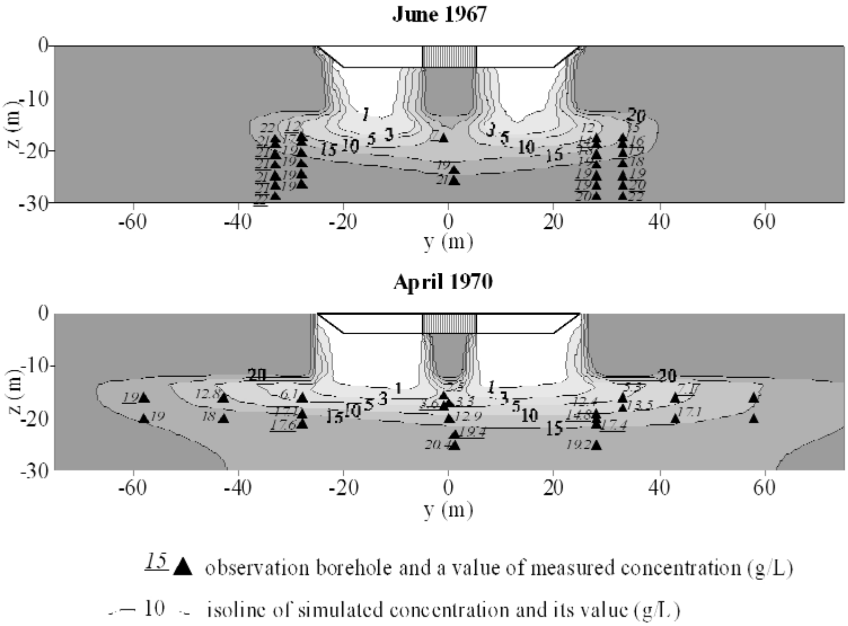

Figure 4. Measured and simulated spatial distribution of concentrations through a vertical cross-section at *x*=0.

and groundwater quality because the cation exchange capacity of sand and clay layers (composing the unsaturated zone) is small (10-30 meq/kg for sand, and up to 120 meq/kg for clay). The dissolution-precipitation of gypsum may increase groundwater salinity at the initial stages of infiltration. However, after several water infiltration cycles, this effect decreases due to almost complete leaching of salts from the unsaturated zone.

Simulations of the ALFGW for 2-D axi-symmetrical space

To investigate processes of the ALFGW formation and to assess the effect of different parameters on lens extent, a series of simulations for 2-D axi-symmetrical space was carried out. A homogeneous sand profile (radius of 500 m and 30 m depth) was modeled. Saturated hydraulic conductivity, longitudinal and transversal dispersivities were 3 m/day, 1 m and 0.1 m, respectively. Initial groundwater level of 15 m and uniform salt concentration of 20 g/L was prescribed. The sedimentation of particles was not accounted for. A period of 10 years was analyzed, assuming that throughout the first 5 years, 5000 m^3 of water was infiltrated through the pond (radius of 25 and 20 m at the top and at the bottom, respectively, and of 3 m depth) during the first month of each year. The second 5 years period was simulated subject to the conditions that the ALFGW was not replenished. Figures 5a depict the distribution of concentration, flow velocity vectors and streamline patterns for the end of the 5th year. We note that at the lens edges, the water flow has a vortex pattern. This behavior is due to differences in densities of fresh and saline water. The ALFGW that is not replenished (Figures 5b) decreases in thickness with a rate of about 90 cm/year, while increases into a lateral extent by 1.6 m/year. After 5 years, the thickness of the transition zone between fresh and saline water (a zone between iso-concentrations of 1 and 10 g/L) in vertical direction

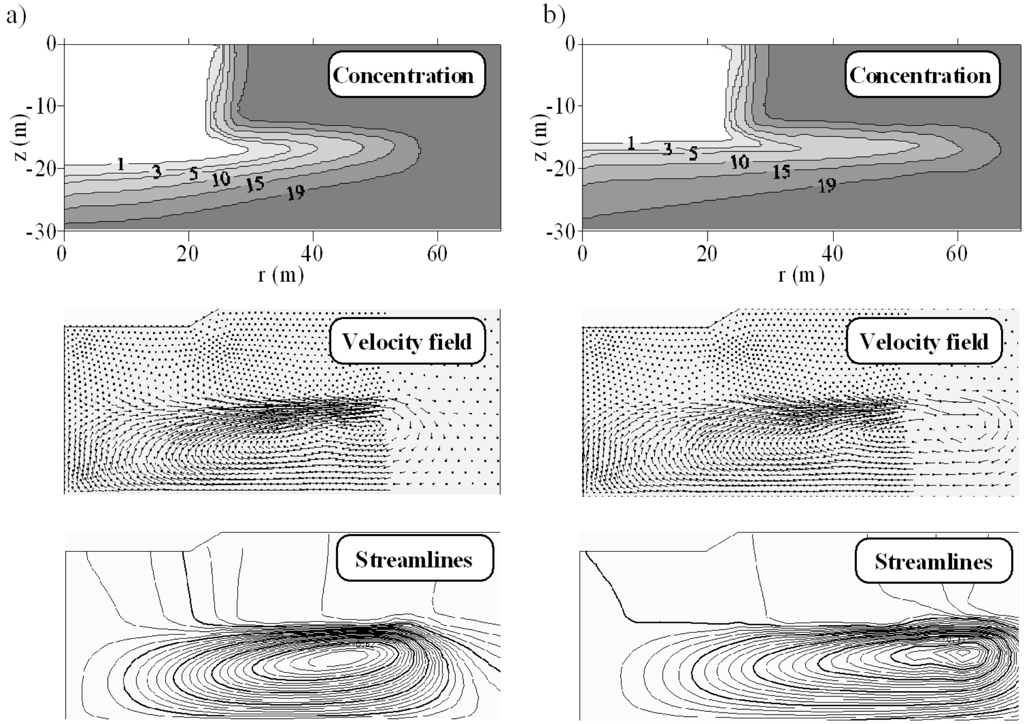

Figure 5. Simulated distributions of concentration (g/L), velocity field and streamlines: after 5 years of 5000 m^3 ALFGW replenishment per year; after additional 5 years without the ALFGW replenishment.

decreases from 5 to 4 m. While horizontally this zone increased from 19 to 31 m. The reason of such behavior is vortex flow below the lens. Close to the middle of the ALFGW, the flow velocities directed upward and solute dispersive flux has the same direction, reducing the lens thickness. Away from the center of the lens, flow in the transition zone is mainly horizontal and opposite to the direction of the dispersive flux, increasing lens width. With time, the vortex center moves in a horizontal direction to the lens edges.

Sensitivity analysis was performed to assess the effect of physical parameters on the ALFGW extension. The following parameters were changed during simulations: saturated hydraulic conductivity; longitudinal and transversal dispersivities; initial groundwater salinity; infiltration basin configuration; and groundwater depth. A water volume of 25,000 m^3 was infiltrated through the pond boundary surface during 5 years (5,000 m^3/year).

It was found that increasing aquifer hydraulic conductivity from 0.5 to 10 m/day lead to a decrease of the ALFGW maximal radius with concentration less than 3 g/l from 34.5 to 29.4 m, while for a concentration less than 10 g/L this radius increases from 40.6 to 45.6 m. For K_s =0.5 m/day the maximal lens thickness was 9.5 and 12.5 m with water salinity of less than 3 to 10 g/L, respectively; while for K_s=10 m/day this thickness was 5.5 and 8.5 m with the same salinity levels.

Increasing longitudinal dispersivity from 0.1 to 2.5 m and transversal dispersivity from 0.01 to 0.1 m, resulted in a decrease of the ALFGW maximal radius from 39.1 to 26.9 m with concentration less than 3 g/L. This radius decreases from 46.9 to 39.2 m for concentration less than 10 g/L. Maximal lens thickness bounded by the isoline of 3 g/L decreases from 8.5 and 5.6 m with the increase of dispersivities. Changing dispersivities does not affect ALFGW thickness with salinity less than 10 g/L.

Simulation with increasing initial groundwater salinity from 20 to 30 g/L indicated that maximum ALFGW radius and thickness decrease by about 3.5 m and 2 m, respectively. Simulations for different configurations of the infiltration pond (radius and depth) demonstrated that the ALFGW volume significantly decreases with an increase of the pond radius. When equal water volume infiltrated over larger area, more water was required for flashing out salts from the unsaturated zone and the developed lens thickness is much smaller. Increasing groundwater depth leads to the same effect of the lens decrease.

Additional simulations were carried out to estimate the effect of infiltration time on the volume of water stored in the ALFGW. Altogether 25,000 m^3 was infiltrated through the pond during 5 years (5000 m^3/year) assuming that the time interval of an infiltration cycle varies for different scenarios. Results indicated that increasing infiltration interval from 5 to 80 days lead to an increase of water volume in the ALFGW with concentrations less than 3 and 10 g/L by about 20% and 30%, respectively. We account this to the flow velocities that decrease in the unsaturated zone with the increase of the infiltration period. Consequently, changes of water table under the pond are much lower, and groundwater velocities are smaller in comparison to the scenario with the short infiltration period. The velocities of the vortex flow, induced by the differences in density of fresh and saline water, are also minor and, therefore, cause a less dispersive flux and a narrower ALFGW mixing zone.

Conclusions

An artificial lens of fresh groundwater (ALFGW) can be created by infiltrating runoff collected during precipitation into the saline groundwater. A mathematical model of density driven flow and transport in the unsaturated-saturated zone was applied to simulate conditions of field experiment conducted at the takyr Karrykul in the southern part of the Kar Kum desert (Leshinsky, 1970). It was found that the infiltration of 26,000 m^3 water during 5 years develops the ALFGW with a radius of 45 m, a thickness of 4.5 m, and a water volume of 5,200 m^3 with salinity less than 10 g/L.

Simulations of the ALFGW indicated that with time, a vortex flow is being developed under the lens edges. This leads to an increase of the mixing between the fresh and saline water zones, thus, decreasing the lens areal extent and thickness. The process mainly depends on the hydraulic parameters of the aquifer and the water infiltration regime. Lowering hydraulic conductivity and infiltration rate lead to an increase of the ALFGW. However, increase of infiltration time raises water losses by evaporation.

Future work will concentrate on simulating different pumping scenarios of the ALFGW.

Acknowledgments

This research was supported under Grant No. TA-MOU-01-CA20-035 funded by the U.S.-Israel Cooperative Development Research Program, Bureau for Economic Growth, Agriculture, and Trade, U.S. Agency for International Development.

References

ARYA, L.M. and PARIS, J.F. (1981). A physicoempirical model to predict moisture characteristics from particle size distribution and bulk density data., *Soil Sci. Soc. Am. J.,* 45: 1023-1030.

BURGER, R., CONCHA, F. and KARLSEN, K. H. (2001). Phenomenological model of filtration processes:1. Cake formation and expression. *Chemical Engineering Science*, 56: 4537-4553

DAM, J.C. van, (1999). Exploitation, Restoration and Management., Ch. 4 in: BEAR, J., CHENG, A.H.-D., SOREK, S., OUAZAR, D. and I. HERRERA (Eds.) "*Seawater Intrusion in Coastal Aquifers-Concepts, Methods and Practices*"., Kluwer, Dordrecht: 73-125.

DIERSCH, H.-J.G. (2002). FEFLOW Reference Manual., WASY, Berlin, 78p.

GANUS, G. A. and KUZNETSOV, M.Ya. (1992). Models for designing artificial lenses of fresh groundwater. *Problems of Desert Development*, 4: 61-65.

KUNIN, V.N. (1959). Local water of the desert and problems of their use. Moscow: 1- 283 (in Russian).

LEBBE, L.C. (1983). Mathematical model of the evolution of the fresh water lens under the dunes and the beach with semi-diurnal tides., *Geologia Applicata e Idrogeologia*, 18(2): 211-226.

LESHINSKY, G.T. (1970). On a rational use of temporary runoff for watering pastures in the desert. ILIM, Ashkhabad, Turkmenistan: 1-50 (in Russian).

MAMIEVA, I.D. (1999). The technology of making lenses of fresh undergrounds water in deserts. in: "*Desert Problems and Desertification in Central Asia*î. (Ed. BABAEV A.G.), Springer: 189-199.

MISHRA, S., PARKER, J.C., and SINGHAl, N. (1989). Estimation of soil hydraulic properties and their uncertainty from particle size distribution data., *J. Hydrol.*, 108: 19-33.

ROGOVSKAYA, N.V., VITKOVSKAY, T. P. and KRAVTSOV, G.K. (1986). The quantitative aspect of assessment of fresh groundwater resources supplied by infiltration. *Problems of Desert Development*, 2: 69-75.

VAN GENUCHTEN, M.Th. (1980). A closed-form equation for predicting the hydraulic conductivity of the unsaturated soils., *Soil Sci. Soc. Am. J.,* 44, 892-899.

WENTWORTH, C.K. (1948). Progress in the estimating of ground-water supplies in Hawaii. *Trans. Amer. Geoph. Union*, 28(2).

YAKIREVICH A., BERLINER, P. and SOREK, S. (1997). A model for numerical simulation of evaporation from bare saline soil. *Water Resources Research*, 33(5): 1021-1033.